Clinical Cancer Research

SLFN11 Is a Transcriptional Target of EWS-FLI1 and a Determinant of Drug Response in Ewing Sarcoma

Sai-Wen Tang[1], Sven Bilke[2], Liang Cao[2], Junko Murai[1], Fabricio G. Sousa[1,3], Mihoko Yamade[1], Vinodh Rajapakse[1], Sudhir Varma[1], Lee J. Helman[4], Javed Khan[2], Paul S. Meltzer[2], and Yves Pommier[1]

Abstract

Purpose: SLFN11 was identified as a critical determinant of response to DNA-targeted therapies by analyzing gene expression and drug sensitivity of NCI-60 and CCLE datasets. However, how *SLFN11* is regulated in cancer cells remained unknown. Ewing sarcoma, which is characterized by the chimeric transcription factor EWS-FLI1, has notably high *SLFN11* expression, leading us to investigate whether EWS-FLI1 drives *SLFN11* expression and the role of SLFN11 in the drug response of Ewing sarcoma cells.

Experimental Design: Binding sites of EWS-FLI1 on the *SLFN11* promoter were analyzed by chromatin immunoprecipitation sequencing and promoter-luciferase reporter analyses. The relationship between *SLFN11* and EWS-FLI1 were further examined in EWS-FLI1-knockdown or -overexpressing cells and in clinical tumor samples.

Results: EWS-FLI1 binds near the transcription start site of *SLFN11* promoter and acts as a positive regulator of *SLFN11* expression in Ewing sarcoma cells. EWS-FLI1–mediated *SLFN11* expression is responsible for high sensitivity of Ewing sarcoma to camptothecin and combinations of PARP inhibitors with temozolomide. Importantly, Ewing sarcoma patients with higher *SLFN11* expression showed better tumor-free survival rate. The correlated expression between *SLFN11* and *FLI1* extends to leukemia, pediatric, colon, breast, and prostate cancers. In addition, expression of other ETS members correlates with *SLFN11* in NCI-60 and CCLE datasets, and molecular experiments demonstrate that ETS1 acts as a positive regulator for *SLFN11* expression in breast cancer cells.

Conclusions: Our results imply the emerging relevance of *SLFN11* as an ETS transcription factor response gene and for therapeutic response to topoisomerase I inhibitors and temozolomide–PARP inhibitor combinations in ETS-activated cancers. *Clin Cancer Res; 21(18); 4184–93. ©2015 AACR.*

See related commentary by Kovar, p. 4033

Introduction

The family of *Schlafen* genes (*SLFN*), which is only found in mammals, has been reported to regulate several key biologic functions including cell-cycle arrest, differentiation, and cancer cell invasion (1–3). In addition, SLFN11 was recently discovered as a dominant response factor of cancer cells to topoisomerase I inhibitors (4, 5). Knockdown of SLFN11 increases chemoresistance of cancer cells to a broad range of DNA-damaging agents (4, 6), and ectopic expression of SLFN11 sensitizes colon cancer cells to topoisomerase I inhibitors (7), consistent with the involvement of SLFN11 in the DNA damage response (4). Concurrently, David and colleagues demonstrated an antihuman immunodeficiency virus-1 (HIV-1) function of SLFN11 due to replication inhibition by selective suppression of viral protein synthesis in a codon usage–dependent manner (8). The emerging relevance of SLFN11 in cancer biology and therapeutic responses incited us to investigate how *SLFN11* expression is regulated in cancer cells.

Ewing sarcoma is a malignant tumor primarily occurring in bones or soft tissues of children and young adults. It readily metastasizes to other organs including the lungs, bones, and bone marrow (9). The overall survival of Ewing sarcoma patients remains poor; 25% of patients with localized tumor and 75% of patients with metastasis do not have durable therapeutic responses (9, 10). Approximately 85% of Ewing sarcoma are characterized by the chromosome translocation (11;22)(q24;q12) encoding the chimeric transcription factor EWS-FLI1 comprising the amino-terminal transactivation domain of EWSR1 fused to the carboxy-terminal ETS DNA-binding domain of FLI1 (11). FLI1 is a member of the family of ETS transcription factors containing a highly conserved domain that recognizes ETS core consensus sites (GGAA/T); the flanking DNA sequence providing the affinity and specificity (12, 13). EWS-FLI1 is oncogenic by regulating multiple target genes through binding to typical ETS core consensus sites or GGAA microsatellites (14, 15). Moreover, EWS-FLI1 is able to colocalize with E2F3 on proximal promoters to activate target genes (16).

Ewing sarcoma cells expressing EWS-FLI1 have been shown to be remarkably sensitive to the inhibitors of PARP (17). Emerging studies suggest that PARP inhibitors combined with temozolomide show significant synergism in Ewing sarcoma cells (18, 19), with the combination inducing more cytotoxic PARP–DNA

[1]Laboratory of Molecular Pharmacology, Developmental Therapeutics Branch, NCI, NIH, Bethesda, Maryland. [2]Genetics Branch, NCI, NIH, Bethesda, Maryland. [3]CETROGEN, PPGFARM, UFMS, Campo Grande, Brazil. [4]Pediatric Oncology Branch, Center for Cancer Research, NCI, NIH, Bethesda, Maryland.

Note: Supplementary data for this article are available at Clinical Cancer Research Online (http://clincancerres.aacrjournals.org/).

Corresponding Author: Yves Pommier, NIH/NCI, 37 Convent Drive, Room 5068, Bethesda, MD 20892-4255. Phone: 301-496-5944; Fax: 301-402-0752; E-mail: pommier@nih.gov

doi: 10.1158/1078-0432.CCR-14-2112

Translational Relevance

DNA-damaging agents, such as topoisomerase I inhibitors, are widely used for the treatment of human cancers. Emerging studies suggest the synergistic effects of inhibitors of PARP combined with temozolomide for treating Ewing sarcoma. Recently, SLFN11 has been suggested as a predictor for the sensitivity of cancer cells, and importantly SLFN11 is capable of sensitizing cancer cells to DNA-damaging agents. Here, we show that *SLFN11* expression is transcriptionally activated by ETS transcription factors EWS-FLI1 and ETS1. *SLFN11* may be a prognostic marker for the tumor-free survival of Ewing sarcoma patients. Our results further show that EWS-FLI1–activated *SLFN11* expression sensitizes Ewing sarcoma cells to camptothecin and PARP inhibitors plus temozolomide combinations, suggesting the emerging relevance of SLFN11 for the sensitivity of ETS-overexpressing cancer to DNA-damaging agents.

complex than either single agent (20, 21). In addition, Barretina and colleagues showed that Ewing sarcoma cell lines with high *SLFN11* are highly sensitive to topoisomerase I inhibitors (5). Motivated by these findings, we hypothesized that EWS-FLI1 plays a role in the expression of *SLFN11* and the response of Ewing sarcoma cells to camptothecin and the combinations of PARP inhibitor plus temozolomide. In the current study, we demonstrate a direct role of EWS-FLI1 as a positive transcriptional regulator of *SLFN11*, and implicate SLFN11 in the sensitivity to topoisomerase I inhibitor and the synergistic effects of PARP inhibitors plus temozolomide in relationship with EWS-FLI1 expression. We further extend *SLFN11* regulation by another ETS transcription factor ETS1 in breast and other cancers.

Materials and Methods

Cells, plasmids, and drugs

293T and A673 cells were maintained in DMEM supplemented with 10% FBS, 2 mmol/L L-glutamine and antibiotics in 5% CO_2 at 37°C. HT1080/GFP, HT1080/EWS-FLI1, and Hs 343.T cells were maintained in RPMI supplemented with 10% FBS, 2 mmol/L L-glutamine, 4 μg/mL balsticidin, and antibiotics in 5% CO_2 at 37°C. A673 cells with doxycycline-inducible shRNA targeting EWS-FLI1 (ASP14) were kindly provided from Dr. Heinrich Kovar (22) and maintained in DMEM with 10% FBS, 2 mmol/L L-glutamine, 2 μg/mL balsticidin, 50 μmol/L Zeocin, and antibiotics in 5% CO_2 at 37°C. pCB6/EWS-FLI1–expressing plasmid was a gift from Dr. Suzanne Baker. pCMV6-ETS1–expressing plasmid was obtained from OriGene. Drugs were obtained from the NCI Drug Developmental Therapeutics Program (DTP).

Chromatin immunoprecipitation sequencing data analysis

The ChIP-Seq dataset for the chromosome binding region of EWS-FLI1 in A673 Ewing sarcoma cell line were obtained as described in a previous study (16). The tag data from ChIP-Seq analysis were uploaded to the Integrative Genomics Viewer from UCSC (http://www.genome.ucsc.edu) and the tag density of EWS-FLI1 binding near the transcription start site (TSS) of *SLFN11* was analyzed.

ETS-binding motif prediction

The potential ETS-binding sites in EWS-FLI1 binding region of *SLFN11* promoter (33,700,532−33,700,847) were predicted using the JASPAR database, including the DNA-binding patterns of transcription factors and other sequence-specific DNA binding proteins (http://jaspar.genereg.net; refs. 23, 24). The predicted sites with a relative score more than 0.9 were considered as the potential ETS-binding sites.

Construction of human *SLFN11* promoter

The *SLFN11* promoter between −840 bp upstream and +460 bp downstream of TSS) was amplified by PCR with the primers (forward, 5′-TTTCTCTATCGATAGGTACCAGTGCGGCATTAACCGCTGCT-3′; reverse, 5′-ACGCGTAAGAGCTCGGTACCCGGACAGGGGAGAAAAGCACA-3′), and cloned into pGL3-basic luciferase reporter vector following the manufacturer's instructions (In-Fusion HD Cloning Kit; Clontech Laboratories, Inc.). The three potential EWS-FLI1 binding sites were mutated using QuikChange II XL Site-Directed Mutagenesis Kit according to the manufacturer's instructions (Stratagene). The primers used to introduce mutations were: mt+91: 5′-TCGCGGGCTTAGCAGACCTATACATTGGCTCTTGCATCTCC-3′; mt+181: 5′-ACCTGGGCGCCTCCAGCATGACGCTAAGGGGGCTTC-3′; mt+201, 5′-ACGCTAAGGGGGCTTCCATGGCGCTGGAGCTTGAGAG-3′. All constructs were verified by nucleotide sequencing.

Promoter-luciferase reporter assay

Cells were cotransfected with pGL3-*SLFN11* promoter plasmid and pCMV-β-galactosidase plasmid using Lipofectamine 2000 Transfection Reagent according to the manufacturer's instructions (Life Technologies). After transfection for 24 hours, luciferase activity was assayed by the luciferase assay kit (Promega) and β-galactosidase activity was determined by the Tropix Galacto-Star chemiluminescent reporter gene assay (Applied Biosystems) following the manufacturer's instructions. The luminescent signal was measured by the EnVision 2104 Multilabel Reader (PerkinElmer). β-Galactosidase activity was the internal control of transfection efficiency for the normalization of luciferase activity.

Quantitative real-time PCR

The cells were washed with PBS twice, and total RNAs were extracted using TRIzol reagent (Invitrogen) and reverse transcribed to complementary DNA by SuperScript II Reverse Transcriptase kit (Invitrogen) according to the manufacturer's instructions. The primers used to amplify specific gene were as follows: *SLFN11* (forward 5′-GGCCCAGACCAAGCCTTAAT-3′ and reverse 5′-CACTGAAAGCCAGGGCAAAC-3′), *FLI1* (forward 5′-CCAAAGTGCACGGCAAAAGA-3′ and reverse 5′-GGCATGGTAGGAAGGCATGT-3′) and *GAPDH* (forward 5′-TCAACGACCACTTTGTCAAGCT-3′ and reverse 5′-GTGAGGGTCTCTCTCTTCCTCTTGT-3′). Quantitative real-time PCR was carried out with FastStart Universal SYBR Green Master (Roche Applied Science) by the 7900HT Fast Real-Time PCR System (Applied Biosystems) according to the manufacturer's instructions. The melting curve was generated to confirm the amplification specificity. *GAPDH* was used as the internal control. The relative level of gene expression was determined using the $2^{(-\Delta\Delta C_t)}$ method.

Western blotting

Cells were washed with PBS twice and then lysed in 50 mmol/L Tris-HCl, pH 7.5, 150 mmol/L NaCl, 5 mmol/L EDTA, 1% Triton

X-100, 0.1% SDS supplemented with protease inhibitor cocktail (Roche). The lysates were separated in 8% of SDS-PAGE and transferred to polyvinylidene fluoride membranes (Millipore). Immunoblotting was performed with antibodies specific to SLFN11 (sc-374339, Santa Cruz Biotechnology), FLI1 (sc-356, Santa Cruz Biotechnology), GSK3β (610201, BD Transduction Laboratories), or actin (MAB1501, Chemicon International), followed by horseradish peroxidase–conjugated secondary antibodies (GE Healthcare Life Sciences). Actin was used as the loading control.

Microarray and RNA-seq data

The whole-genome expression profile analyses of the NCI-60 (CellMiner tools: http://discover.nci.nih.gov/cellminer) and CCLE (http://www.broadinstitute.org/ccle/home) cell lines were recently described (5, 25). The gene expression profiles of 44 Ewing sarcoma tumor samples and 18 normal skeletal muscle tissues by microarray analysis (26) were downloaded from the Gene Expression Omnibus website (GSE17674, http://www.ncbi.nlm.nih.gov/geo; ref. 27). The raw signal intensities were normalized by Robust Multichip Average (RMA) method and Log2-transformed. The median-normalized expression of *SLFN11* and *FLI1* in the dataset of 163 pediatric cancers was obtained from Pediatric Preclinical Testing Program (http://home.ccr.cancer.gov/oncology/oncogenomics; ref. 28). The RNA-Seq data for gene expression in the datasets of colon, breast, and prostate cancers were retrieved from TCGA portal (http://cancergenome.nih.gov).

siRNA transfection and cell viability assay

Cells were transfected with 10 nmol/L of *SLFN11*-targeting, *ETS1*-targeting, or nontargeting siRNAs (Thermo Scientific Dharmacon) using Lipofectamine 2000 Transfection Reagent according to the manufacturer's instructions (Life Technologies). After transfection for 1 day, cells were treated as indicated. Cell viability was measured by MTS assay (Promega). The cell viability was calculated by setting untreated cells as 100%.

Statistical analyses

The two-tailed independent samples *t* test was applied to determine the statistical significance of the differences between the two experimental groups for the promoter-luciferase reporter assay, quantitative real-time PCR, and the cell viability assay. Nonlinear regression was used to calculate the inhibitory concentration 50% (IC_{50}) of camptothecin. The association between the expression levels of two individual genes in a dataset was evaluated by the Pearson correlation, and where multiple comparisons were made, the *P* values were adjusted using the Bonferroni method. The Kaplan–Meier curves based on *SLFN11* expression higher or lower than the median in the cohort of 44 Ewing sarcoma patients (26) were analyzed using the Mantel–Cox log-rank test. The test results with $P < 0.05$ were considered to be statistically significant unless otherwise stated.

Results

EWS-FLI1 binds to and activates the *SLFN11* promoter

To determine whether EWS-FLI1 regulates *SLFN11*, we analyzed the results of ChIP-Seq analysis from Ewing sarcoma A673 cells (16) by focusing on the *SLFN11* promoter region. Notably, preferential binding of EWS-FLI1 was found at the TSS of *SLFN11* (Fig. 1A). To determine whether EWS-FLI1 directly activates *SLFN11* transcription, we cloned the promoter region of *SLFN11* (from −840 to +460 bp from the TSS), and performed promoter-luciferase reporter assays. For these experiments, we used the EWS-FLI1–overexpressing HT1080 cells (HT1080/EWS-FLI1) and GFP-expressing cells (HT1080/GFP) as reference control (29). The results showed that the induction of *SLFN11* promoter activity was selectively enhanced in HT1080/EWS-FLI1 cells, but not in the HT1080/GFP control cells (Fig. 1B). In addition, transient expression of EWS-FLI1 in 293T cells significantly enhanced *SLFN11* promoter activity (Fig. 1C). These results indicate that EWS-FLI1 binds to and activates the *SLFN11* promoter.

Next, we analyzed the *cis*-acting sequence responsible for EWS-FLI1–mediated regulation of the *SLFN11* promoter. The EWS-FLI1 ChIP-Seq data showed the highest sequence tag density in EWS-FLI1 binding sites on the *SLFN11* promoter, approximately at genomic position 33,700,733 on chromosome 17, which is 91 bp downstream from the *SLFN11* TSS (Fig. 1A, +91 bp). In addition, two potential ETS core consensus sites (+181 bp, +201 bp from the TSS) were annotated by JASPAR, the open-access database of transcription factor binding motif (23, 24). To determine the relative contribution of these putative FLI1 binding site(s) to the EWS-FLI1-induced *SLFN11* promoter activity, we tested 3 *SLFN11* promoter mutations by site-directed mutagenesis (mt+91, mt+181, mt+201). Luciferase reporter assays showed that individual mutations at positions +91 and +201 reduced *SLFN11* promoter activity by more than 80%, whereas the +181 mutation had no significant effect (Fig. 1D). *SLFN11* promoter activity in 293T/EWS-FLI1 cells was also suppressed by approximately 90% for mt+91 and 50% for mt+201, whereas mt+181 did not affect *SLFN11* promoter activity (Fig. 1E). These results indicate that consensus sequences +91 and +201 are critical for activation of the *SLFN11* promoter by EWS-FLI1.

EWS-FLI1 regulates the expression of *SLFN11*

To demonstrate that EWS-FLI1 activates endogenous *SLFN11*, SLFN11 mRNA and protein levels were examined in HT1080/EWS-FLI1 and HT1080/GFP cells by quantitative real-time PCR and Western blotting analyses (Fig. 2A and B). HT1080/EWS-FLI1 cells displayed significant higher SLFN11 both at the mRNA and protein levels than HT1080/GFP cells. To confirm the regulation of *SLFN11* expression by EWS-FLI1, we used the ASP14 cell line, which is derived from the A673 cells, but contain a doxycycline-inducible shRNA targeting *EWS-FLI1* (22). The results showed that doxycycline significantly decreased both *EWS-FLI1* and *SLFN11* expression in ASP14 cells, but not in the parent A673 cells not expressing the *EWS-FLI1* shRNA (Fig. 2C and D). On the basis of these results, we conclude that EWS-FLI1 transcriptionally regulates the expression of *SLFN11*.

SLFN11 expression is correlated with *FLI1* expression and may predict tumor-free survival in Ewing sarcoma patients

Next, we tested the correlations between *FLI1* and *SLFN11* expression using gene expression microarray data of Ewing sarcoma tumor samples and normal skeletal muscle tissues (26, 30). As shown in Fig. 3A, *FLI1* and *SLFN11* expressions were significantly correlated ($r = 0.83$, $P < 0.0001$). We also examined the correlation between *FLI1* and *SLFN11* expression in a cohort of pediatric cancer samples including primary tumors, xenograft, and cell line samples of Ewing sarcoma, rhabdomyosarcoma, osteogenic sarcoma, acute lymphoblastic

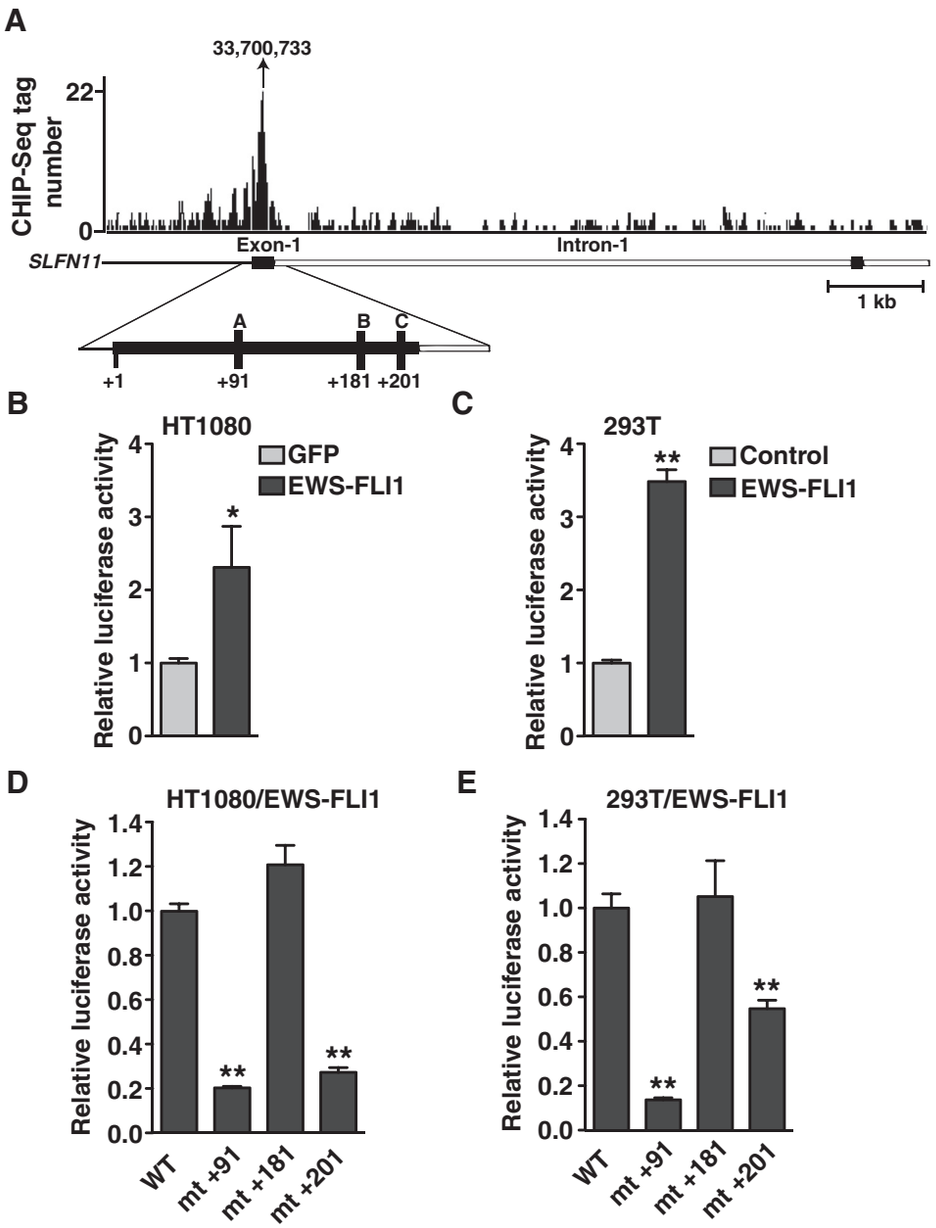

Figure 1.
Activation of the *SLFN11* promoter by EWS-FLI1. A, ChIP-Seq tag density plot for EWS-FLI1 on *SLFN11* promoter. The arrow indicates the highest tag density (chromosome 17, 33,700,733, +91 bp from the TSS, site A). Black boxes represent exons. Potential ETS core consensus sites (sites B and C at positions +181 and +201 bp) were predicted by JASPAR (http://jaspar.genereg.net). B, HT1080 cells stably expressing EWS-FLI1 (dark gray) or GFP (light gray) were transfected with pGL3-*SLFN11* promoter for 24 hours before measuring luciferase activity. The *y*-axis represents the promoter activity relative to control (GFP). C, 293T cells were transfected with *SLFN11* promoter plus EWS-FLI1–expressing plasmid (dark gray) or *SLFN11* promoter plus an empty control plasmid (light gray) for 24 hours before measuring luciferase activity. The *y*-axis represents the promoter activity relative to control (Control). D, HT1080/EWS-FLI1 were transfected with the wild-type *SLFN11* promoter (WT) or mutated *SLFN11* promoters (mt+91, mt+181 or mt+201) for 24 hours before measuring luciferase activity. E, 293T cells were transfected with EWS-FLI1–expressing plasmid plus the wild-type *SLFN11* promoter (WT) or mutated *SLFN11* promoters (mt+91, mt+181 or mt+201) for 24 hours before measuring luciferase activity. Representative results in triplicate from three independent experiments are shown as mean ± SD. *, $P < 0.05$; **, $P < 0.001$ by *t* test.

leukemia (ALL), brain cancers, and Wilms' tumor from the NCI Pediatric Preclinical Testing Program (http://home.ccr.cancer.gov/oncology/oncogenomics; ref. 28). *FLI1* and *SLFN11* expression levels were highly correlated in 163 samples of pediatric cancers ($r = 0.68$, $P < 0.0001$; Fig. 3B). Ewing sarcoma and ALL, which express high *EWS-FLI1* and *FLI1*, respectively, showed the strongest *SLFN11* expression (Fig. 3B). Brain cancers and rhabdomyosarcoma displayed a strong correlated expression of *FLI1* and *SLFN11* (Fig. 3B).

We also evaluated whether *SLFN11* expression might be a prognostic marker for the tumor-free survival of Ewing sarcoma patients. The patients were divided into two groups by *SLFN11* higher or lower than median expression and analyzed by log-rank test. Ewing sarcoma patients with higher *SLFN11* expression exhibited better prognosis than those with lower *SLFN11* expression ($P = 0.0046$, HR = 3.17, 95% CI, 1.43–7.05; Fig. 3C).

EWS-FLI1–mediated SLFN11 expression determines DNA damage response

Because SLFN11 expression sensitizes cells to DNA-damaging agents (4, 5, 7), we tested the impact of EWS-FLI1–mediated *SLFN11* expression on the sensitivity of Ewing sarcoma cells to camptothecin, a specific topoisomerase I inhibitor whose derivatives irinotecan and topotecan are widely used in the anticancer armamentarium (31). We found that doxycycline-induced EWS-FLI1 downregulaton significantly reduced the sensitivity of ASP14 cells to camptothecin

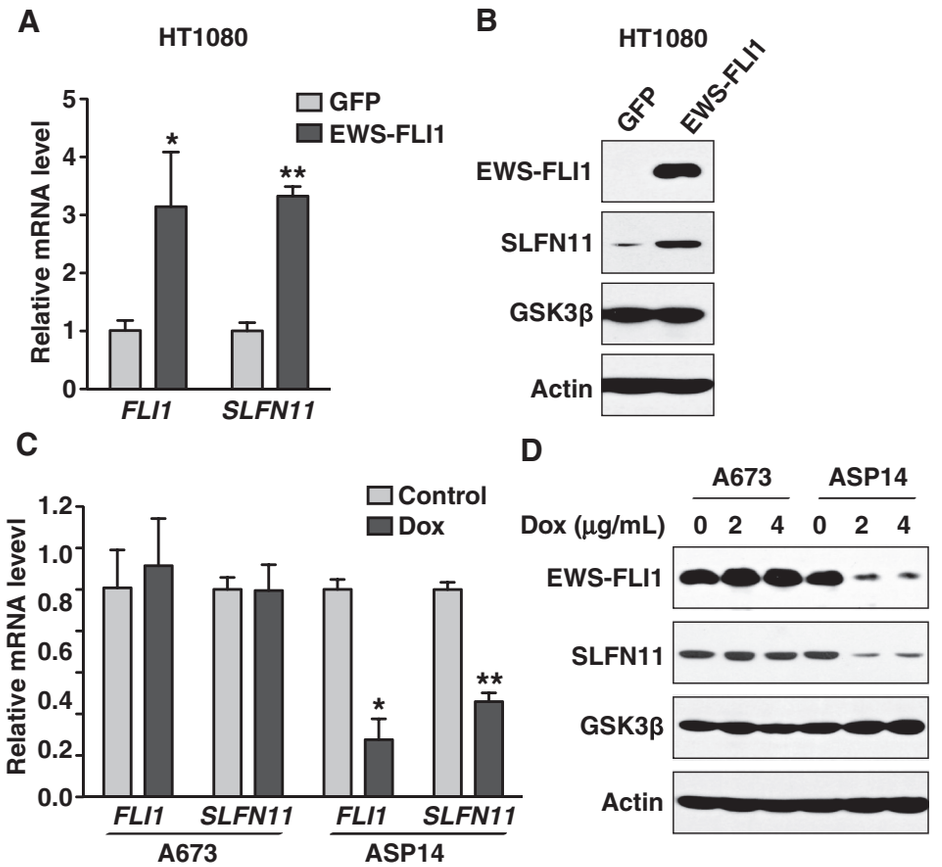

Figure 2.
Regulation of SLFN11 expression by EWS-FLI1. A, mRNA levels of *EWS-FLI1* and *SLFN11* in HT1080/EWS-FLI1 and HT1080/GFP were measured by quantitative real-time PCR. The *y*-axis represents the relative expression normalized to HT1080/GFP control. B, protein levels of EWS-FLI1 and SLFN11 in HT1080/EWS-FLI1 and HT1080/GFP determined by Western blotting using antibodies against FLI1 (EWS-FLI1, 68 kDa), SLFN11 (98 kDa), GSK-3β (46 kDa), or actin (42 kDa, the loading control). C, mRNA levels of *EWS-FLI1* and *SLFN11* in A673 or ASP14 cells treated with or without (control) doxycycline (Dox, 2 μg/mL) for 4 days. The *y*-axis represents relative expression normalized to control. Representative results in triplicate from three independent experiments are shown as mean ± SD. *, $P < 0.05$; **, $P < 0.001$ by *t* test. D, protein levels of EWS-FLI1 and SLFN11 in A673 or ASP14 cells treated with or without doxycycline (Dox, 2 or 4 μg/mL) for 4 days.

(IC_{50} = 94 nmol/L vs. 17 nmol/L in the presence and absence of doxycycline, respectively; Fig. 4A). Similarly, transfection of A673 cells with *SLFN11* siRNA increased resistance to camptothecin (IC_{50} = 75 nmol/L vs. 10 nmol/L in the presence and absence of *SLFN11* siRNA, respectively; Fig. 4B). Conversely, HT1080/EWS-FLI1 cells were more sensitive to camptothecin than HT1080/GFP cells (IC_{50} = 0.29 μmol/L vs. 0.85 μmol/L, respectively; Fig. 4C), and *SLFN11* knockdown in HT1080/EWS-FLI1 cells counteracted EWS-FLI1–induced sensitivity to camptothecin in comparison with control siRNA-transfected

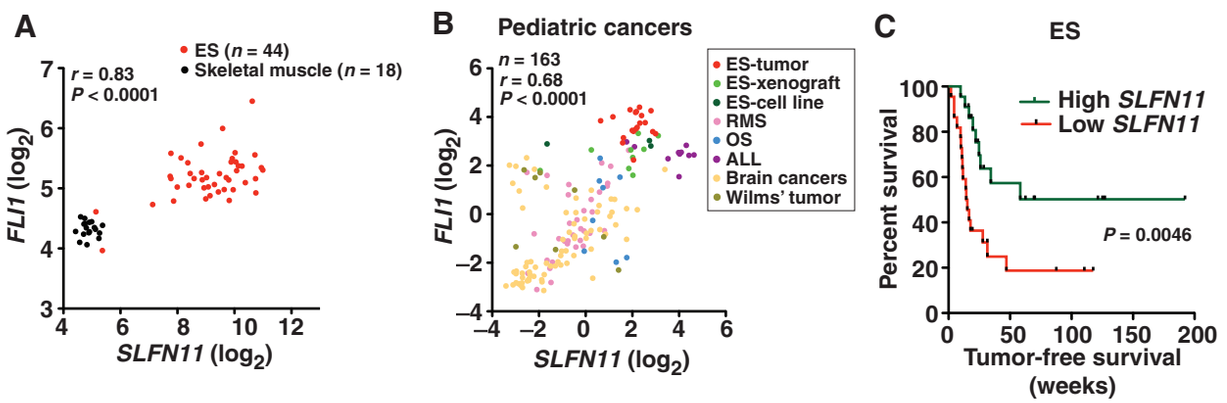

Figure 3.
SLFN11 expression is positively correlated with *FLI1* expression and tumor-free survival in clinical Ewing sarcoma samples. A, scatterplot showing positive correlation between *SLFN11* expression (x axis, Log_2 normalized intensity) and *FLI1* expression (y axis, Log_2 normalized intensity) from the microarray dataset of 44 Ewing sarcoma tumor samples and 18 normal skeleton muscle tissues. *r*, correlation coefficient. B, scatterplot showing the positive correlation between *SLFN11* (*x*-axis, median-centered log_2 normalized intensity) and *FLI1* expression (*y*-axis, median-centered log_2 normalized intensity) in 163 pediatric cancer samples. C, Kaplan–Meier curves of 44 Ewing sarcoma patients. Patients are stratified with respect to *SLFN11* expression level (above or below median). Abbreviations: RMS, rhabdomyosarcoma; OS, osteogenic sarcoma.

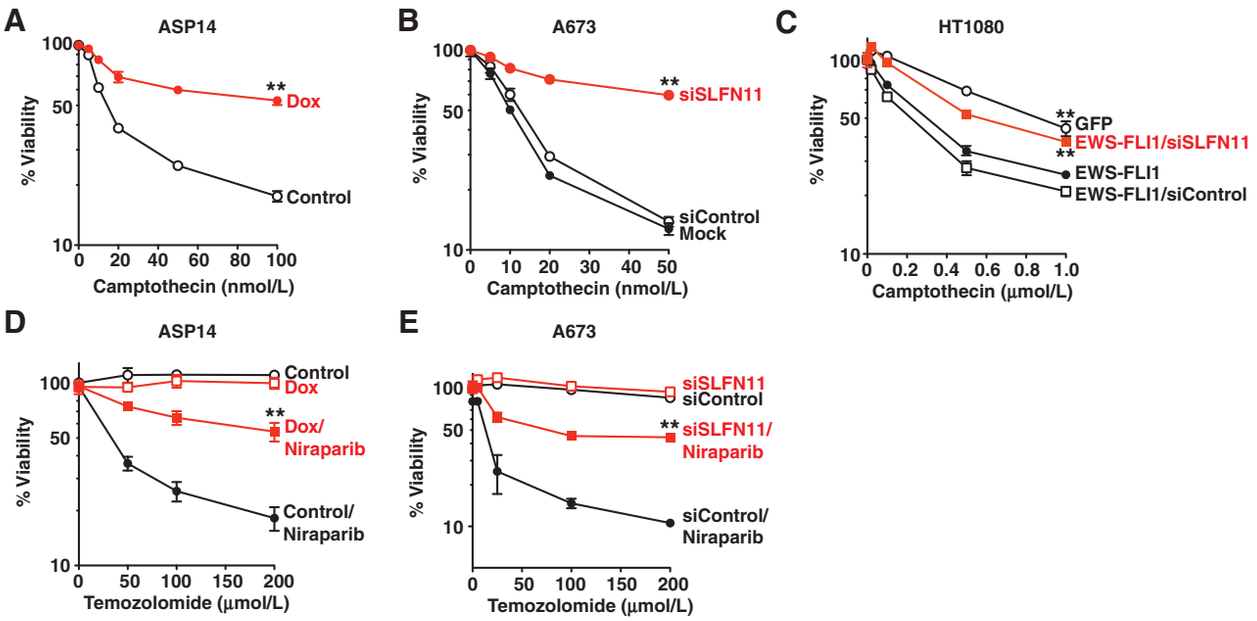

Figure 4.

Role of EWS-FLI1–mediated *SLFN11* expression in the response to camptothecin and in the synergistic effect of niraparib and temozolomide. A, ASP14 cells preincubated with doxycycline (Dox, 2 μg/mL; red solid circles) or without doxycycline (control, open circles) were treated with camptothecin for 2 days before assessing cell viability. B, A673 cells transfected with *SLFN11* siRNA (red solid circle, siSLFN11) or nontargeting siRNA (siControl, black solid circle), or without any siRNA (open circle, mock) were treated with camptothecin for 2 days before assessing cell viability. C, HT1080/GFP (GFP, open circle), HT1080/EWS-FLI1 (EWS-FLI1, black solid circle), HT1080/EWS-FLI1 with nontargeting siRNA (open square, EWS-FLI1/siControl) or HT1080/EWS-FLI1 with *SLFN11* siRNA (red solid square, EWS-FLI1/siSLFN11) were treated with camptothecin for 2 days before measuring cell viability. D, ASP14 cells were preincubated with or without doxycycline (Dox and Control, respectively), and then were treated with niraparib (1 μmol/L) plus temozolomide (doxycycline/niraparib, Control/niraparib) or with temozolomide only (Control, Dox) for 2 days before assessing cell viability. E, A673 cells transfected with *SLFN11* siRNA (siSLFN11) or nontargeting siRNA (siControl), and then were treated with niraparib (1 μmol/L) plus temozolomide (siSLFN11/niraparib, siControl/niraparib) or with temozolomide only (siSLFN11, siControl) for 2 days before assessing cell viability. Untreated cells were set as 100%. Representative results in triplicate from three independent experiments are shown as mean ± SD. **, $P < 0.001$ by *t* test.

HT1080/EWS-FLI1 cells (IC_{50} = 0.62 μmol/L vs. 0.19 μmol/L, respectively; Fig. 4C).

We further evaluated the role of SLFN11 in the synergistic effects of the combination of PARP inhibitors plus temozolomide. ASP14 and A673 cells were relatively insensitive to single agent temozolomide (50–200 μmol/L) or niraparib (1 μmol/L), while the combination of niraparib and temozolomide killed ASP14 and A673 cells efficiently (Fig. 4D and E). ASP14 cells with EWS-FLI1 knockdown and A673 cells with *SLFN11* knockdown exhibited resistance to the combination of niraparib plus temozolomide (Fig. 4D and E). These findings demonstrate that the upregulation of *SLFN11* by EWS-FLI1 enhances the sensitivity of Ewing sarcoma cells to camptothecin and plays a role in the synergistic effects of PARP inhibitors with temozolomide.

FLI1 and *SLFN11* coexpression in other types of cancers

We next examined the correlation of *FLI1* and *SLFN11* in other types of cancers. By analyzing the gene expression dataset of 1,036 cancer cell lines from the Broad Insitute (the Cancer Cell Line Encyclopedia, CCLE; ref. 5), we observed that the majority of ALL, acute myeloid leukemia, and chronic myeloid leukemia cell lines showed a strong correlated expression between *FLI1* and *SLFN11* (Fig. 5A). We also evaluated the expression of *FLI1* and *SLFN11* in tumor samples of colon, breast, and prostate cancers obtained from the gene expression datasets of The Cancer Genome Atlas (TCGA). The results showed that *FLI1* and *SLFN11* expression are highly correlated across 233 colon cancers (Fig. 5B; $r = 0.62$, $P < 0.0001$), 994 breast cancers (Fig. 5C; $r = 0.45$, $P < 0.0001$), and in 195 prostate cancers (Fig. 5D; $r = 0.19$, $P = 0.007$). Together, these results imply that FLI1 regulates *SLFN11* expression not only in Ewing sarcoma but also in other pediatric cancers, leukemia, colon, breast, and prostate cancers.

ETS1 and *SLFN11* coexpression in breast cancer and prostate cancer

To examine whether other ETS transcription factors (12) might regulate *SLFN11* expression, we tested the correlation between the expression levels of 27 ETS members and *SLFN11* in the NCI-60 cancer cell lines (CellMiner tools: http://discover.nci.nih.gov/cellminer; refs. 25, 32). *ETS1*, *FLI1*, *ETV4*, and *EHF* showed a significant correlation with *SLFN11* expression in the gene expression dataset of the NCI-60 cancer cell line panel (Table 1; $|r| > 0.43$, $P < 0.05$). Extension of correlation analysis of ETS members with *SLFN11* in the CCLE dataset revealed significant correlation of *FLI1*, *ETS1*, *ERG*, *SPI1*, *ELF3*, *ETV4*, and *EHF* with *SLFN11* (Table 1; $|r| > 0.20$, $P < 0.01$). *ETS1* also exhibited a strong positive correlation with *SLFN11* in the TCGA datasets of breast cancers (Fig. 5E; $r = 0.43$, $P < 0.0001$), and prostate cancers (Fig. 5F; $r = 0.54$, $P < 0.0001$).

Promoter-luciferase reporter analyses were performed to test the causality between ETS1 and *SLFN11* expression. Figure 6

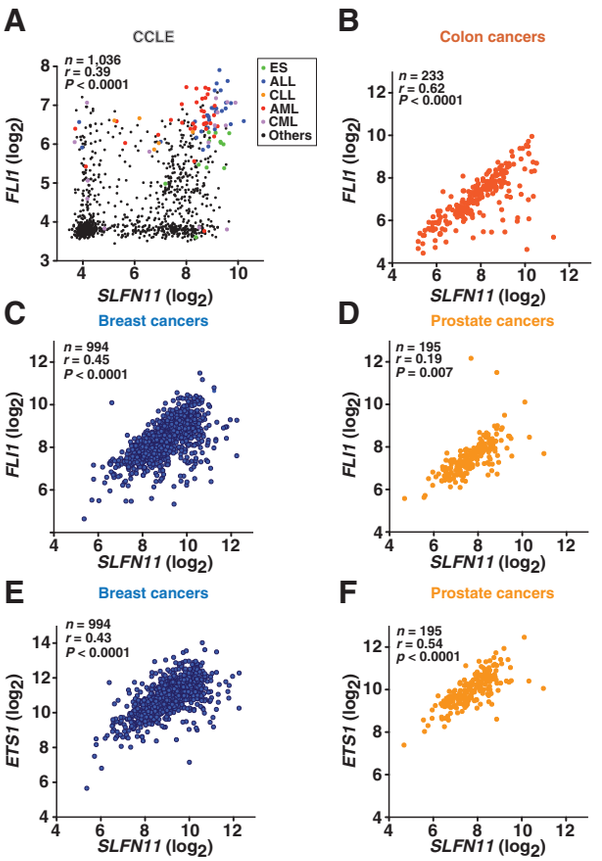

Figure 5.
Correlation between *SLFN11* and *FLI1* expression in the Broad Institute cancer cell line panel (CCLE) and between *SLFN11* and *FLI1* and *ETS1* in clinical tumor samples. Scatterplots show the positive correlation between *SLFN11* (*x*-axis, $\log_2$ normalized intensity) and *FLI1* expression (*y*-axis, $\log_2$ normalized intensity) in the cancer cell lines from the CCLE dataset (A), in TCGA samples of colon, breast and prostate cancers (B–D). E and F, correlations between *SLFN11* (*x*-axis, log2 normalized intensity) and *ETS1* expression (*y*-axis, log2 normalized intensity) in breast and prostate cancers from TCGA. n, number of samples; *r*, correlation coefficient. Abbreviations: CLL, chronic lymphocytic leukemia; AML, acute myeloid leukemia; CML, chronic myelogenous leukemia.

Table 1. Correlation analysis of ETS family members with SLFN11 expression in the gene expression datasets of NCI-60 and CCLE

NCI60[a]		CCLE[a]	
Gene symbol	Correlation coefficient	Gene symbol	Correlation coefficient
ETS1	0.44[b]	*FLI1*	0.39[c]
FLI1	0.43[b]	*ETS1*	0.22[c]
ETV6	0.37	*ERG*	0.21[c]
ELK3	0.33	*SPI1*	0.20[c]
ERG	0.23	*ETV6*	0.18
ERF	0.21	*ELF2*	0.18
ELK4	0.20	*ELK3*	0.16
ELF2	0.20	*GABPA*	0.15
GABPA	0.11	*ELF1*	0.13
ELF4	0.08	*ELK4*	0.10
SPI1	0.06	*ELF4*	0.09
ETV1	0.03	*SPIC*	0.06
ETV5	0.01	*ETS2*	0.05
ETS2	−0.03	*ETV5*	0.03
ELK1	−0.07	*SPIB*	0.03
ELF1	−0.07	*ETV7*	0.03
ETV7	−0.09	*ELK1*	0.00
ELF5	−0.13	*ETV1*	−0.03
SPIC	−0.13	*FEV*	−0.03
SPDEF	−0.23	*ETV2*	−0.08
ETV3	−0.24	*ELF5*	−0.09
ETV2	−0.26	*ETV3*	−0.09
FEV	−0.29	*ERF*	−0.10
ELF3	−0.34	*SPDEF*	−0.16
SPIB	−0.41	*EHF*	−0.25[c]
EHF	−0.43[c]	*ETV4*	−0.25[c]
ETV4	−0.44[c]	*ELF3*	−0.26[c]

[a]ETS genes are ranked by decreasing Pearson correlation coefficient.
[b]Pearson $|r| > 0.43$, $P < 0.05$ (Bonferroni-adjusted).
[c]Pearson $|r| > 0.20$, $P < 0.01$ (Bonferroni-adjusted).

shows that ETS1 was able to activate the *SLFN11* promoter in 293T cells (Fig. 6A). Moreover, *SLFN11* promoter activity was decreased by mutating the ETS consensus sequences within the *SLFN11* promoter (see Fig. 1). The mutant mt+91 showed an approximately 80% reduction and the mt+201 mutant approximately 60% reduction (Fig. 6B), indicating that positions +91 and +201 in the *SLFN11* promoter are important for ETS1-mediated activation of *SLFN11*. Finally, siRNA-mediated *ETS1* knockdown suppressed SLFN11 expression at the RNA and protein levels and resulted in resistance to camptothecin treatment in breast cancer cell line Hs 343.T (Fig. 6C–E). These results are consistent with a role of ETS1 in the regulation of *SLFN11* expression and sensitivity to topoisomerase I inhibitors in breast cancer.

Discussion

Recent studies revealed that high SLFN11 expression enhances the response of cancer cells to a broad range of DNA-damaging agents (4, 5, 7). Yet, until the current study, there was no information on the regulation of *SLFN11* in cancer cells (33). Our study implicates EWS-FLI1 as a causative regulator for *SLFN11* expression in Ewing sarcoma. Unlike *SLFN11*, we found that the other 3 human *Schlafen* genes *SLFN5*, *SLFN12*, and *SLFN13* are not strongly correlated with *FLI1* expression in the NCI-60 and CCLE datasets, indicating that FLI1 specifically regulates the expression of *SLFN11*, but not the expression of the other *SLFN* genes in spite of their common location on human chromosome 17q12 (2).

Our study also demonstrates the involvement of EWS-FLI1–induced *SLFN11* expression in the response of Ewing sarcoma cells to camptothecin and to the combination of PARP inhibitors with temozolomide, suggesting that cancers with higher *SLFN11* expression might be more sensitive to DNA-damaging agents. Ewing sarcoma tumors initially respond to chemotherapy; however, 30% of patients relapse with relatively less sensitivity to chemotherapies and less than 20% long-term survival rate (34). Thus, further studies are warranted to investigate whether the expression or function of SLFN11 is suppressed in relapsed Ewing sarcoma tumors.

EWS-FLI1 has been considered as a therapeutic target for the treatment of Ewing sarcoma. Knockdown of *EWS-FLI1* by antisense cDNA or siRNA suppresses the growth and invasiveness of Ewing sarcoma cells (35, 36). Recently, trabectedin, a marine alkaloid that alkylates DNA at guanine N2 and poisons transcription-coupled repair (37, 38) has been demonstrated to interfere with the activity of EWS-FLI1 and to reverse EWS-FLI1–mediated gene expression signatures (29). In addition, trabectedin showed

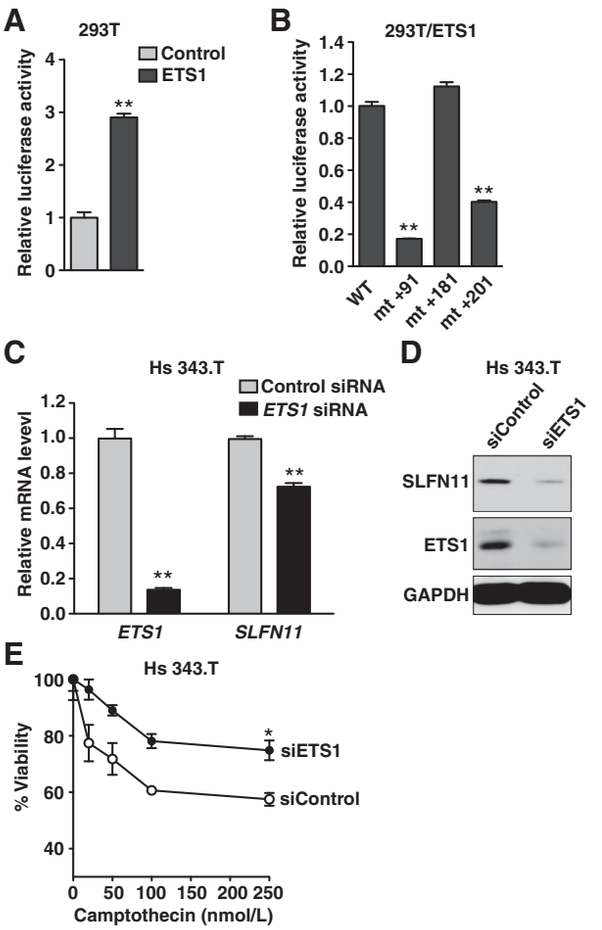

Figure 6.

Regulation of *SLFN11* expression by ETS1. A, 293T cells were transfected with a luciferase plasmid under *SLFN11* promoter plus an ETS1-expressing plasmid (dark gray) or plus an empty control plasmid (light gray) for 24 hours before measuring luciferase activity. The *y*-axis represents the promoter activity relative to control (Control). B, 293T cells were transfected with ETS1-expressing plasmid plus wild-type *SLFN11* promoter (WT) or mutated *SLFN11* promoters (mt+91, mt+181 or mt+201) for 24 h before measuring luciferase activity. C, mRNA levels of *ETS1* and *SLFN11* in the breast cancer cell line Hs 343.T transfected with *ETS1* siRNA or nontargeting siRNA (Control). The *y*-axis represents relative expression normalized to control. D, protein levels of ETS1 and SLFN11 in Hs 343.T transfected with *ETS1* siRNA or nontargeting siRNA (Control). GAPDH (37 kDa) was used as loading control. E, Hs 343.T cells transfected with *ETS1* siRNA (solid circle, siETS1) or nontargeting siRNA (siControl, solid circle) were treated with camptothecin for 2 days before assessing cell viability. Representative results in triplicate from three independent experiments are shown as mean ± SD. *, $P < 0.05$; **, $P < 0.001$ by *t* test.

a synergic effect with the clinical camptothecin derivative SN-38 in Ewing sarcoma cells by inhibiting EWS-FLI1–mediated expression of Werner syndrome helicase, whose deficiency causes cellular hypersensitivity to camptothecins (39, 40). Our experiments demonstrate that knockdown of *EWS-FLI1* downregulates *SLFN11* expression, and consequently reduces the sensitivity of cancer cells to camptothecin and the combinations of PARP inhibitor temozolomide. Hence, developing SLFN11-activating agents could be viewed as a rationale for combinatorial therapy to enhance the efficacy of DNA-damaging agents. According to our unpublished data, the demethylating agent azacytidine was able to reactivate *SLFN11* expression in cancer cells with methylated *SLFN11* promoter, providing an avenue to activate SLFN11 expression in the clinical setting.

Besides EWS-FLI1, chromosome translocations (21;22)(q22;q12), which fuse EWSR1 with another ETS transcription factor ERG1 (EWS-ERG), were found in about 5%–10% of Ewing sarcoma (41–43). Both ERG and FLI1 belong to ERG subfamily in ETS transcription factor family with similar DNA-binding domains (12). To understand whether SLFN11 expression is also activated in EWS-ERG–expressing cells, we compared SLFN11 levels in 25 Ewing sarcoma cell lines with EWS-FLI1 and 4 Ewing sarcoma cell lines with EWS-ERG, and found that SLFN11 expression showed no difference between EWS-FLI1 and EWS-ERG–expressing cells (Supplementary Fig. S1). Another chromosome translocation, which encodes a fusion protein TMPRSS2-ERG, was found in approximately 40% of prostate cancer (44). Interestingly, when analyzing the TCGA prostate cancer dataset, we did not observe a significant correlation between *SLFN11* and *ERG* (data not shown) indicating that activation of *SLFN11* expression might require other proteins besides ETS transcription factors.

In this study, we also identified ETS1, like FLI1, as a dominant activator of *SLFN11* expression in breast cancer. ETS1 has been shown to play an important role in the progression of breast cancer (45) and has been recently linked to the RAS/ERK pathway in carcinomas (46). Bonetti and colleagues recently demonstrated that FLI1 and ETS1 cooperatively contribute to the growth of diffuse large B-cell lymphoma, and influence gene expression related to germinal center differentiation (47). In addition, due to the chromosome gene region of *FLI1* and *ETS1* are closely adjacent, the 11q24.3 gain might result in FLI1 and ETS1 expression in diffuse large B-cell lymphoma (47). Our findings reveal that both *FLI1* and *ETS1* are highly correlated with *SLFN11* expression in both datasets of the NCI-60 and CCLE, as well as the datasets of breast, colon, and prostate cancers from TCGA. We also observed a positive correlation between the expression levels of *FLI1* and *ETS1* in the datasets of breast and prostate cancers (Supplementary Fig. S2). Further studies are warranted to understand how FLI1 and ETS1 are coregulated or regulate each other.

In conclusion, our findings reveal an unsuspected connection between *SLFN11* and the ETS transcription factors, which are commonly upregulated in cancer and autoimmune diseases. Our study also highlights the potential importance of SLFN11, FLI1 and ETS1 as predictive genomic biomarkers for DNA-damaging agents and combinations of PARP inhibitors with temozolomide.

Disclosure of Potential Conflicts of Interest

No potential conflicts of interest were disclosed.

Authors' Contributions

Conception and design: S.-W. Tang, L. Cao, J. Murai, M. Yamade, L.J. Helman, Y. Pommier

Development of methodology: F.G. Sousa, Y. Pommier

Acquisition of data (provided animals, acquired and managed patients, provided facilities, etc.): S.-W. Tang, F.G. Sousa, J. Khan, Y. Pommier

Analysis and interpretation of data (e.g., statistical analysis, biostatistics, computational analysis): S.-W. Tang, S. Bilke, L. Cao, F.G. Sousa, M. Yamade, V. Rajapakse, S. Varma, L.J. Helman, P.S. Meltzer, Y. Pommier

Writing, review, and/or revision of the manuscript: S.-W. Tang, S. Bilke, L. Cao, J. Murai, J. Khan, P.S. Meltzer, Y. Pommier

Administrative, technical, or material support (i.e., reporting or organizing data, constructing databases): Y. Pommier
Study supervision: Y. Pommier

Acknowledgments

The authors thank Dr. Heinrich Kovar (Children's Cancer Research Institute, St. Anna Kinderkrebsforschung, Vienna, Austria) for providing the A673 cells with doxycycline-inducible shRNA targeting EWS-FLI1, and Dr. Suzanne Baker (Department of Developmental Neurobiology, St. Jude Children's Research Hospital, Tennessee) for the EWS-FLI1-expressing plasmid.

Grant Support

This work was supported by the Center for Cancer Research, Intramural NCI program (Z01 BC 006150).

The costs of publication of this article were defrayed in part by the payment of page charges. This article must therefore be hereby marked *advertisement* in accordance with 18 U.S.C. Section 1734 solely to indicate this fact.

Received August 14, 2014; revised January 26, 2015; accepted March 4, 2015; published OnlineFirst March 16, 2015.

References

1. Bustos O, Naik S, Ayers G, Casola C, Perez-Lamigueiro MA, Chippindale PT, et al. Evolution of the Schlafen genes, a gene family associated with embryonic lethality, meiotic drive, immune processes and orthopoxvirus virulence. Gene 2009;447:1–11.
2. Mavrommatis E, Fish EN, Platanias LC. The schlafen family of proteins and their regulation by interferons. J Interferon Cytokine Res 2013;33:206–10.
3. Schwarz DA, Katayama CD, Hedrick SM. Schlafen, a new family of growth regulatory genes that affect thymocyte development. Immunity 1998;9: 657–68.
4. Zoppoli G, Regairaz M, Leo E, Reinhold WC, Varma S, Ballestrero A, et al. Putative DNA/RNA helicase Schlafen-11 (SLFN11) sensitizes cancer cells to DNA-damaging agents. Proc Natl Acad Sci U S A 2012;109:15030–5.
5. Barretina J, Caponigro G, Stransky N, Venkatesan K, Margolin AA, Kim S, et al. The Cancer Cell Line Encyclopedia enables predictive modelling of anticancer drug sensitivity. Nature 2012;483:603–7.
6. Kiianitsa K, Maizels N. A rapid and sensitive assay for DNA-protein covalent complexes in living cells. Nucleic Acids Res 2013;41:e104.
7. Tian L, Song S, Liu X, Wang Y, Xu X, Hu Y, et al. Schlafen-11 sensitizes colorectal carcinoma cells to irinotecan. Anticancer Drugs 2014;25: 1175–81.
8. Li M, Kao E, Gao X, Sandig H, Limmer K, Pavon-Eternod M, et al. Codon-usage-based inhibition of HIV protein synthesis by human schlafen 11. Nature 2012;491:125–8.
9. Balamuth NJ, Womer RB. Ewing's sarcoma. Lancet Oncol 2010;11:184–92.
10. Stahl M, Ranft A, Paulussen M, Bolling T, Vieth V, Bielack S, et al. Risk of recurrence and survival after relapse in patients with Ewing sarcoma. Pediatr Blood Cancer 2011;57:549–53.
11. Delattre O, Zucman J, Plougastel B, Desmaze C, Melot T, Peter M, et al. Gene fusion with an ETS DNA-binding domain caused by chromosome translocation in human tumours. Nature 1992;359:162–5.
12. Hollenhorst PC, McIntosh LP, Graves BJ. Genomic and biochemical insights into the specificity of ETS transcription factors. Annu Rev Biochem 2011;80:437–71.
13. Sharrocks AD. The ETS-domain transcription factor family. Nat Rev Mol Cell Biol 2001;2:827–37.
14. Lessnick SL, Ladanyi M. Molecular pathogenesis of Ewing sarcoma: new therapeutic and transcriptional targets. Annu Rev Pathol 2012;7:145–59.
15. Gangwal K, Sankar S, Hollenhorst PC, Kinsey M, Haroldsen SC, Shah AA, et al. Microsatellites as EWS/FLI response elements in Ewing's sarcoma. Proc Natl Acad Sci U S A 2008;105:10149–54.
16. Bilke S, Schwentner R, Yang F, Kauer M, Jug G, Walker RL, et al. Oncogenic ETS fusions deregulate E2F3 target genes in Ewing sarcoma and prostate cancer. Genome Res 2013;23:1797–809.
17. Garnett MJ, Edelman EJ, Heidorn SJ, Greenman CD, Dastur A, Lau KW, et al. Systematic identification of genomic markers of drug sensitivity in cancer cells. Nature 2012;483:570–5.
18. Brenner JC, Feng FY, Han S, Patel S, Goyal SV, Bou-Maroun LM, et al. PARP-1 inhibition as a targeted strategy to treat Ewing's sarcoma. Cancer Res 2012;72:1608–13.
19. Smith MA, Reynolds CP, Kang MH, Kolb EA, Gorlick R, Carol H, et al. Synergistic activity of PARP inhibition by talazoparib (BMN 673) with temozolomide in pediatric cancer models in the pediatric preclinical testing program. Clin Cancer Res 2015;21:819–32.
20. Murai J, Huang SY, Das BB, Renaud A, Zhang Y, Doroshow JH, et al. Trapping of PARP1 and PARP2 by Clinical PARP inhibitors. Cancer Res 2012;72:5588–99.
21. Murai J, Huang SY, Renaud A, Zhang Y, Ji J, Takeda S, et al. Stereospecific PARP trapping by BMN 673 and comparison with olaparib and rucaparib. Mol Cancer Ther 2014;13:433–43.
22. Carrillo J, Garcia-Aragoncillo E, Azorin D, Agra N, Sastre A, Gonzalez-Mediero I, et al. Cholecystokinin down-regulation by RNA interference impairs Ewing tumor growth. Clin Cancer Res 2007;13:2429–40.
23. Sandelin A, Alkema W, Engstrom P, Wasserman WW, Lenhard B. JASPAR: an open-access database for eukaryotic transcription factor binding profiles. Nucleic Acids Res 2004;32:D91–4.
24. Portales-Casamar E, Thongjuea S, Kwon AT, Arenillas D, Zhao X, Valen E, et al. JASPAR 2010: the greatly expanded open-access database of transcription factor binding profiles. Nucleic Acids Res 2010;38: D105–10.
25. Reinhold WC, Sunshine M, Liu H, Varma S, Kohn KW, Morris J, et al. CellMiner: a web-based suite of genomic and pharmacologic tools to explore transcript and drug patterns in the NCI-60 cell line set. Cancer Res 2012;72:3499–511.
26. Savola S, Klami A, Myllykangas S, Manara C, Scotlandi K, Picci P, et al. High expression of complement component 5 (C5) at tumor site associates with superior survival in ewing's sarcoma family of tumour patients. ISRN Oncol 2011;2011:168712.
27. Barrett T, Troup DB, Wilhite SE, Ledoux P, Rudnev D, Evangelista C, et al. NCBI GEO: archive for high-throughput functional genomic data. Nucleic Acids Res 2009;37:D885–90.
28. Whiteford CC, Bilke S, Greer BT, Chen Q, Braunschweig TA, Cenacchi N, et al. Credentialing preclinical pediatric xenograft models using gene expression and tissue microarray analysis. Cancer Res 2007;67:32–40.
29. Grohar PJ, Griffin LB, Yeung C, Chen QR, Pommier Y, Khanna C, et al. Ecteinascidin 743 interferes with the activity of EWS-FLI1 in Ewing sarcoma cells. Neoplasia 2011;13:145–53.
30. Scotlandi K, Remondini D, Castellani G, Manara MC, Nardi F, Cantiani L, et al. Overcoming resistance to conventional drugs in Ewing sarcoma and identification of molecular predictors of outcome. J Clin Oncol 2009; 27:2209–16.
31. Pommier Y. Drugging topoisomerases: lessons and challenges. ACS Chem Biol 2013;8:82–95.
32. Abaan OD, Polley EC, Davis SR, Zhu YJ, Bilke S, Walker RL, et al. The Exomes of the NCI-60 Panel: A Genomic Resource for Cancer Biology and Systems Pharmacology. Cancer Res 2013;73:4372–82.
33. Katsoulidis E, Mavrommatis E, Woodard J, Shields MA, Sassano A, Carayol N, et al. Role of interferon {alpha} (IFN{alpha})-inducible Schlafen-5 in regulation of anchorage-independent growth and invasion of malignant melanoma cells. J Biol Chem 2010;285:40333–41.
34. Barker LM, Pendergrass TW, Sanders JE, Hawkins DS. Survival after recurrence of Ewing's sarcoma family of tumors. J Clin Oncol 2005;23:4354–62.
35. Kovar H, Aryee DN, Jug G, Henockl C, Schemper M, Delattre O, et al. EWS/FLI-1 antagonists induce growth inhibition of Ewing tumor cells in vitro. Cell Growth Differ 1996;7:429–37.
36. Chansky HA, Barahmand-Pour F, Mei Q, Kahn-Farooqi W, Zielinska-Kwiatkowska A, Blackburn M, et al. Targeting of EWS/FLI-1 by RNA interference attenuates the tumor phenotype of Ewing's sarcoma cells in vitro. J Orthop Res 2004;22:910–7.
37. Pommier Y, Kohlhagen G, Bailly C, Waring M, Mazumder A, Kohn KW. DNA sequence- and structure-selective alkylation of guanine N2 in the DNA minor groove by ecteinascidin 743, a potent antitumor compound from the Carribean tunicate *Ecteinascidia Turbinata*. Biochem 1996;35: 13303–9.

38. Takebayashi Y, Pourquier P, Zimonjic DB, Nakayama K, Emmert S, Ueda T, et al. Antiproliferative activity of ecteinascidin 743 is dependent upon transcription-coupled nucleotide-excision repair. Nat Med 2001;7:961–6.
39. Grohar PJ, Segars LE, Yeung C, Pommier Y, D'Incalci M, Mendoza A, et al. Dual targeting of EWS-FLI1 activity and the associated DNA damage response with trabectedin and sn38 synergistically inhibits ewing sarcoma cell growth. Clin Cancer Res 2014;20:1190–203.
40. Su F, Mukherjee S, Yang Y, Mori E, Bhattacharya S, Kobayashi J, et al. Nonenzymatic role for WRN in preserving nascent DNA strands after replication stress. Cell Rep 2014;9:1387–401.
41. Shulman SC, Katzenstein H, Bridge J, Bannister LL, Qayed M, Oskouei S, et al. Ewing sarcoma with 7;22 translocation: three new cases and clinicopathological characterization. Fetal Pediatr Pathol 2012;31:341–8.
42. Peter M, Couturier J, Pacquement H, Michon J, Thomas G, Magdelenat H, et al. A new member of the ETS family fused to EWS in Ewing tumors. Oncogene 1997;14:1159–64.
43. Sorensen PH, Lessnick SL, Lopez-Terrada D, Liu XF, Triche TJ, Denny CT. A second Ewing's sarcoma translocation, t(21;22), fuses the EWS gene to another ETS-family transcription factor, ERG. Nat Genet 1994;6:146–51.
44. Clark JP, Cooper CS. ETS gene fusions in prostate cancer. Nat Rev Urol 2009;6:429–39.
45. Scheiber MN, Watson PM, Rumboldt T, Stanley C, Wilson RC, Findlay VJ, et al. FLI1 expression is correlated with breast cancer cellular growth, migration, and invasion and altered gene expression. Neoplasia 2014;16:801–13.
46. Plotnik JP, Budka JA, Ferris MW, Hollenhorst PC. ETS1 is a genome-wide effector of RAS/ERK signaling in epithelial cells. Nucleic Acids Res 2014;42:11928–40.
47. Bonetti P, Testoni M, Scandurra M, Ponzoni M, Piva R, Mensah AA, et al. Deregulation of ETS1 and FLI1 contributes to the pathogenesis of diffuse large B-cell lymphoma. Blood 2013;122:2233–41.